Thermally Latent Bases in Dynamic Covalent Polymer Networks and their Emerging Applications

*David Reisinger, Matthias Udo Kriehuber, Marcel Bender, Daniel Bautista-Anguís, Bernhard Rieger and Sandra Schlögl**

D. Reisinger, M. U. Kriehuber, D. Bautista-Anguís, S. Schlögl

Polymer Competence Center Leoben GmbH, Roseggerstraße 12, 8700 Leoben, Austria

E-mail: sandra.schloegl@pccl.at

M. Bender

Processing of Composites Group, Montanuniversität Leoben, Otto Glöckel-Straße 2, 8700 Leoben, Austria

B. Rieger

WACKER-Chair of Macromolecular Chemistry, Technical University of Munich, Lichtenbergstraße 4, 85748 Garching, Germany

Keywords: dynamic covalent polymer networks, vitrimers, low creep, on-demand activation, thermolatent catalysts, 3D printing, composites

A novel strategy allowing a temporal control of dynamic bond exchange in covalently cross-linked polymer networks via latent transesterification catalysts is introduced. Obtained by a straight-forward air- and water-tolerant synthesis, the latent catalyst is designed for an irreversible temperature-mediated release of a strong organic base. Its long-term inactivity at temperatures below 50 °C provides the unique opportunity to equip dynamic covalent networks with creep resistance and high bond exchange rates, once activated. The presented thermally latent base catalyst is conveniently introducible in readily available building blocks and, as proof of concept, applied in a radically polymerized thiol-ene network. Light-mediated curing is used for 3D printing functional objects on which the possibility of spatially controlled reshaping and welding based on dynamic transesterification are illustrated. Since the catalyst is thermally activated, limitations regarding sample geometry and optical transparency do not apply, which facilitates a transfer to well-established industrial technologies. Consequently, fiber-reinforced and highly filled magneto-active thiol-ene polymer composites are fabricated by a thermal curing approach. The on-demand activation of dynamic transesterification is demonstrated by (magneto-assisted) reshaping experiments, highlighting a wide range of potential future applications offered by the presented concept.

1. Introduction

Thermosetting and elastomeric polymers ensure dimensional stability, i.e., creep resistance, as a consequence of their three-dimensional covalently cross-linked network structure even at high operating temperatures. Especially their excellent strength to weight ratio in combination with their chemical resistance renders them attractive for high performance applications, such as structural building parts, protective coatings or sealings.[1–6] Furthermore, covalently cross-linked polymers are widely used as a matrix material for fiber-reinforced composites, particulate composites and laminates. [7]

However, the formation of irreversible crosslinks during polymerization or curing also entails several drawbacks. The manufacturing feasibilities and simplicity of use are considerably limited, as the final shape cannot be adjusted once cured. Moreover, thermomechanical reshaping, welding and recycling processes, commonly employed for thermoplastic polymers, are not applicable.[1–3,8] To address these challenges, especially in terms of resource conservation, strategies for combining the beneficial effects of thermosetting (dimensional stability, chemical resistance) and thermoplastic (repairability, recyclability) polymers have been developed. [4,5,9,10]

So-called vitrimers exhibit a three dimensional covalently cross-linked network structure like thermosetting and elastomeric materials. In response to a specific external trigger (most often heat), however, their network topology can be reorganized through the dynamic exchange of covalent bonds. Owing to an associative bond-forming, bond-breaking reaction sequence, the total number of covalent bonds is preserved independent on the temperature, which improves the material's resistance against creep or solvent stress cracking.[3,9–11] Nonetheless, vitrimers are capable of changing their molecular configuration and thus, are recyclable via thermomechanical processes similar to thermoplastic polymers. [5,12,13]

Different options are available to steer this dynamic behavior and the associated material properties.[14] A precisely defined onset of the exchange reactions, macroscopically observable as a viscoelastic flow according to the Arrhenius law, though, is difficult to realize. Especially with regard to several common industrial applications, dimensional stability and creep resistance are required to be ensured.[15–17] Besides the regulation of available reactants via phase separation or protecting groups and the application of rate-enhancing/inhibiting substituents, latent catalysts are one of the most promising approaches addressing this area of concern, as recently outlined by Du Prez, Winne and coworkers.[17] It is important to note that such a latent catalyst needs to exhibit an (almost) complete inactivity, although a willful activation needs to be as efficient and fast as possible. Moreover, the underlying bond exchange mechanism must be sufficiently slow in the absence of a suitable catalyst for suppressing undesired creep.

In 2018, Bowman et al. introduced the concept of photolatent base catalysts for enabling a controlled – and moreover spatially resolved – activation of thiol-thioester exchange reactions within an elastomeric covalently cross-linked network structure. Through the light-mediated release of a strong guanidine base as an efficient reaction catalyst, they were able to demonstrate an instantaneous onset of dynamic bond exchange at room temperature.[18]

Our research group extended this approach toward the in various polyester networks applicable transesterification mechanism, i.e., the dynamic exchange between hydroxy groups and ester links.[13,19,20] First, a quaternary ammonium salt was incorporated as a photolatent base catalyst in a

crosslinked thiol-epoxy polymer. Demonstrated by stress relaxation measurements, the UV-mediated on-demand release of the strong guanidine base 1,5,7-triazabicyclo[4.4.0]dec-5-ene (TBD) facilitated a reorganization of the network topology provoked by dynamic transesterification.[20] In a follow-up study, we introduced two *N*-substituted derivatives of the amidine base 1,5-diazabicyclo[4.3.0]non-5-ene (DBN) as photolatent catalysts. The moderate residual basicity allocated to the photolatent tertiary amine equipped our thiol-epoxy resin formulation with an ideal thermal curing characteristic.[19] Apart from photolatent bases, we also demonstrated the suitability of various photolatent acids and a photolatent organophosphate for the spatially resolved catalysis of transesterification reactions within a covalently crosslinked thiol-acrylate network structure.[21,22] Whilst photolatent systems benefit from a spatiotemporal catalyst activation in high resolution, considerable shortcomings appear in their practical application.[18,23] Resulting from a limited penetration depth of the light necessary for activation, the spatial object geometry as well as the use of fillers and colorants is severely limited. Moreover, long-term latency of such systems can only be guaranteed under the exclusion of (day)light.

In order to overcome these disadvantages and for achieving maximum freedom in the objects design, we herein expand the concept of latent catalysis for the on-demand activation of dynamic bond exchange in cross-linked polymers from photolatent to thermally latent catalysts. The development of a suitable thermally latent base catalyst, including an efficient synthesis procedure and analysis of the cleavage reaction, is described. Incorporated in a thiol-ene resin system, curing is achieved by means of radical photoinitators or low temperature radical initiators. Stress relaxation and creep experiments highlight an outstanding change in the bond exchange rate and related mechanical behavior through the thermally induced on-demand release of a strong guanidine base. Additionally, several applications, such as the permanent reshaping of covalently crosslinked magnetic nanocomposites and fiber-reinforced composites as well as the (spatially resolved) reshaping and welding of 3D-printed objects demonstrate the salient features of our system compared to the established light-activated systems.

2. Results and Discussion

2.1. Development of a Thermally Latent Base Catalyst

In the development/synthesis of an appropriate thermally latent base catalyst, the main focus was placed on quaternary ammonium salts. These compounds represent one of the very limited possibilities to equip tertiary amines, known as one of the most efficient transesterification catalysts, with a thermal latency.[13,24,25] For the presented concept, schematically illustrated in **Figure 1a-c**, the further restriction of an irreversible latency applies. Meaning that after one-time thermal activation, the amine base remains catalytically active regardless of the temperature. In order to meet this condition within our polymeric matrix system, the stabilizing anion needs to decompose during the activation process without damaging the amine base or the network structure containing ester links and hydroxy groups.

For photolatent bases, light-mediate decarboxylation of quaternary ammonium carboxylates accompanied by the irreversible release of tertiary amines is an established concept.[23,26,27] Tsang and coworkers complementarily outlined that the salt generated between 1,5,7-triazabicyclo[4.4.0]dec-5-ene (TBD) and 2-(3-benzoylphenyl)propanoic acid (ketoprofen) can also decarboxylate solely thermally and thus, release TBD in an irreversible manner.[24] Based on the fact that ketoprofen is still light sensitive, expensive and toxic, it is herein replaced by an alternative carboxylic acid.[23,27,28] In the literature, it has been known for decades that cyanoacetic acid (CA) undergoes thermal decarboxylation at temperatures around 160 °C.[29–31] Moreover, even the cyanoacetate anion is able to decarboxylate at elevated temperatures, rendering this compound an ideal candidate.[32,33] In a straight-forward air- and water-tolerant one-step synthesis between TBD and CA, the corresponding quaternary ammonium salt 1,5,7-triazabicyclo[4.4.0]dec-5-enylcyanoacetate (TBD-CA) was obtained in 95 % of the theoretical yield as a colorless solid (Figure 1a).

To verify the synthesis and proposed structure for TBD-CA, ^{1}H and ^{13}C NMR spectra were recorded. For unconverted TBD, signals at 3.01 ppm (H_a, H_c and H_d) and 1.73 ppm (H_b) can be observed. After the formation of TBD-CA, the separate signal for H_d disappears due to protonation of the adjacent nitrogen atom. The signals originating from H_a, H_b and H_c are shifted toward slightly higher values to 3.15, 1.87 and 3.25 ppm, respectively (**Figure 1d**). Moreover, the broad -OH peak of CA (13.36 ppm) is absent and the original -NH peak of TBD (4.63 ppm) is shifted to 9.52 ppm in the ^{1}H NMR spectrum of TBD-CA. Full-scale ^{1}H and ^{13}C NMR spectra for TBD, CA as well as the synthesized TBD-CA are

provided in **Figure S1-3**. According to the literature, all the observations described confirm the formation of a quaternary ammonium salt composed of TBD in its protonated state as the cationic and a carboxylate as the anionic part.[34]

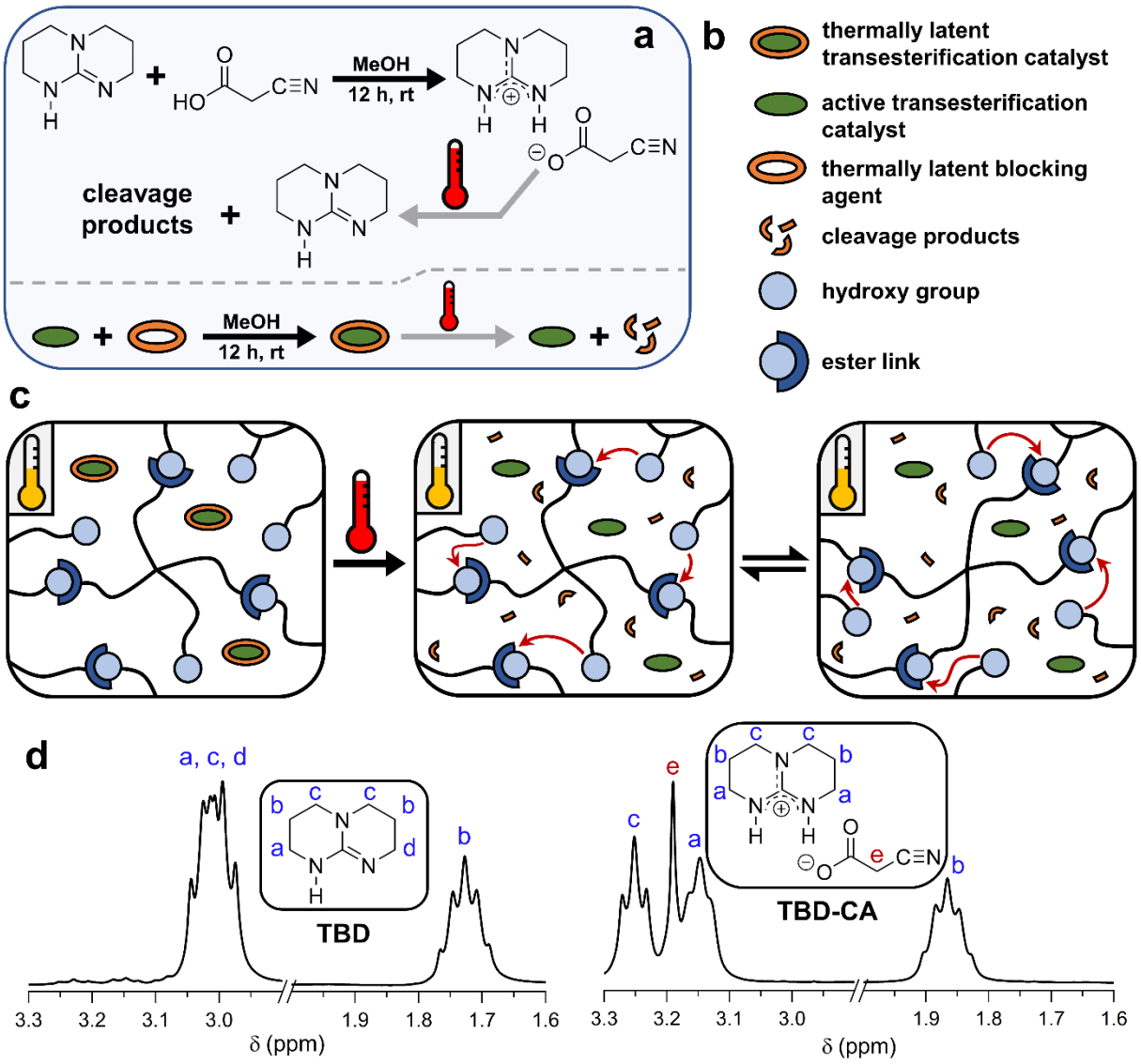

Figure 1. a) Molecular and schematic representation of the one-step synthesis of TBD-CA followed by the on-demand thermally inducible and irreversible activation process under the release of TBD. b) Legend explaining the schematic symbols used. c) Schematic representation of the heat-triggered and irreversible activation of the thermally latent transesterification catalyst enabling the dynamic exchange between ester links and hydroxy groups within a cross-linked polymer network. d) Methylene region of the ^{1}H NMR spectra of TBD and TBD-CA.

2.1.1. Thermal Activation of TBD-CA

For monitoring the thermally induced activation of TBD-CA, i.e., decomposition of the cyanoacetate anion accompanied by the irreversible release of TBD, an on-line combination of thermogravimetric analysis followed by gas phase FTIR spectroscopy (TGA-FTIR) was used (**Figure 2a**-**f**). All measurements were performed under nitrogen atmosphere at a heating rate of 20 °C min^{-1}. Moreover, complementary evolved gas analysis mass spectrometry (EGA-MS) measurements were carried out (**Figure 3a-c**).

In a first step, the thermal behavior of the unreacted educts was analyzed. For CA, as thermolabile blocking agent, a considerable mass loss (more than 2.5 wt%) can be determined at about 140 °C (Figure 2a). The first distinct absorption signal in the IR spectra of the escaping gases (Figure 2b) observable at 150 °C can be assigned to CO_2 (2334 cm^{-1}). These observations agree with the literature reporting the decomposition of CA between 140 and 160 °C under the release of CO_2 and acetonitrile.[29–31] Due to the low intensity of the IR absorption signals originated from acetonitrile, its release is hard to detect via TGA-FTIR.[30] From 175 °C onwards, apart from decomposition, evaporation of intact monomeric CA molecules with a characteristic carbonyl stretching band at 1797 cm^{-1} can be observed.[31,35] At a later stage (above 200 °C), a shift toward slightly lower wavenumbers (1751 cm^{-1}) induced by a gas phase dimerization, typical for small carboxylic acids, appears. Stretching vibrations of the related acidic hydroxy groups are most likely visible at 3579 (monomeric CA) and 3430 cm^{-1} (dimeric CA), although a definite assignment is hampered by overtone and combination bands occurring in this wavenumber region (Figure 2b).[35,36]

In comparison, TBD shows the same mass loss of 2.5 wt% at about 150 °C (Figure 2c). At this temperature, also the first IR-active signals resulting from the released gases appear. Except for the basic intensity, no significant changes in the spectrum occur over the entire temperature range (Figure 2d). According to the literature, the main characteristic bands corresponding to N-H stretching (3442 cm^{-1}), C-H stretching (3043-2745 cm^{-1}) and asymmetric C=N stretching modes (1655 cm^{-1}) can be assigned to intact TBD.[37,38] As the catalytically active species, TBD exhibits the imperatively required higher thermal stability compared to CA. In addition, within the polymeric matrix under investigation, volatilization of intact TBD starting at about 150 °C is only of minor importance.

The synthesized quaternary ammonium salt TBD-CA reaches the initial mass loss of 2.5 wt% at about 130 °C (Figure 2e), which is around 10 °C lower compared to unconverted CA (Figure 2a). Furthermore, a significant change in the rate of mass loss is noticeable at about 150 °C. The 37 wt% lost up to this temperature correspond to the theoretical mass fraction of CA (38 wt%). FTIR analysis of the escaping gases confirm the decomposition of the cyanoacetate anion by a pronounced signal at 2334 cm^{-1} originated from CO_2.[30,31] Onwards from a temperature of 150 °C, mainly the non-destructive evaporation of TBD with the same characteristic absorption bands as in the analysis of pure TBD (3442 cm^{-1}, 3043-2745 cm^{-1} and 1655 cm^{-1}) is detected (Figure 2f).[37,38]

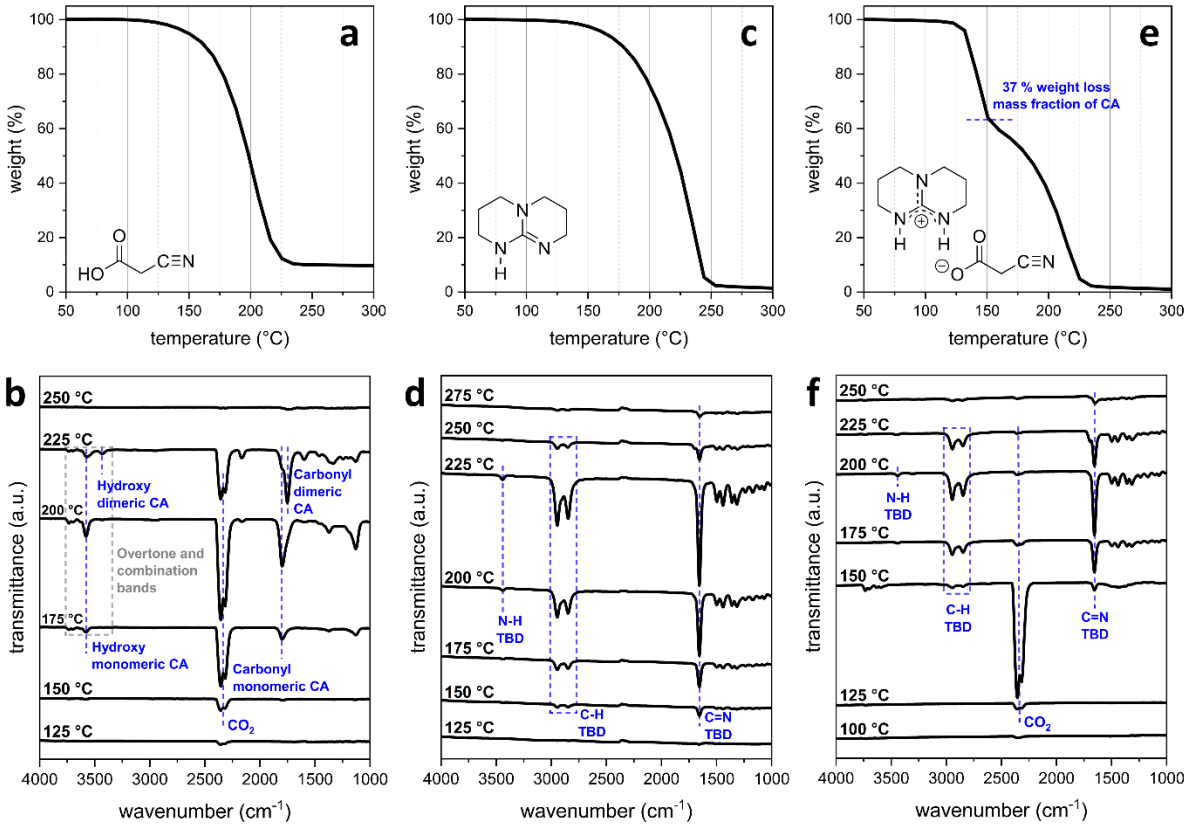

Figure 2. a, c, e) TGA-FTIR data including the thermogravimetric analysis of the reactants CA (a) and TBD (c) together with the synthesized quaternary ammonium salt TBD-CA (e). b, d, f) Corresponding FTIR spectra from 1000 up to 4000 cm^{-1} of the escaping gases originated from CA (b), TBD (d) and TBD-CA (f) are shown in intervals of 25 °C.

It is important to note that the identification of a merely thermally induced complete decomposition of the cyanoacetate anion is of essential importance with respect to an irreversible release of the catalytically active TBD and the underlying concept (Figure 1a-c). EGA-MS further strengthened the results and interpretations based on TGA-FTIR. Consistent with Figure 2e, the total ion thermogram (TIT) of TBD-CA shows a two-step decomposition process with a change in rate at about 156 °C (Figure 3a). The concurrent release of acetonitrile along with CO_2 as well as the subsequent volatilization of intact TBD (pronounced peak tailing) are observable in the normalized thermal evolution profile of these compounds' molecular ion peaks $[M]^+$ (Figure 3b). However, due to the fact that the m/z ratios for CO_2 (m/z 44) and acetonitrile (m/z 41) are also among the ionization products of TBD, a precise separation between both processes is considerably more complicated to identify than by TGA-FTIR. The described behavior is also evident from the mass spectra recorded at 100, 150, 170 and 250 °C (Figure 3c). All detected signals higher than m/z 44 can be attributed to the ionization process of intact TBD.[39] For a more detailed insight, **Figure S4** shows mass spectra in narrower temperature intervals. In addition, the TIT and the corresponding evolution profiles of the m/z ratios 41, 44 and 139 of a repeat measurement are provided in **Figure S5**. The raw data of both measurements can be found in the supporting information.

In comparison to the analysis of free CA (Figure 2b), the CO_2 release period is significantly shorter for TBD-CA. Moreover, the vaporization of intact acid molecules, with pronounced carbonyl signals at 1797 cm^{-1} (monomeric) and 1751 cm^{-1} (dimeric), is not observable via TGA-FTIR (Figure 2f).[35] Both are clear indications of an altered decomposition mechanism and allow an exclusion of the back formation of free CA from the quaternary ammonium salt. In the literature, the decarboxylation of cyanoacetates is basically described to proceed via direct decarboxylation of the anion itself. As a result, a resonance-stabilized acetonitrile carbanion is generated.[30,32,33,40] In the decarboxylation process of TBD-CA, this carbanion is instantaneously protonated by the cationic TBD, as indicated by the precisely simultaneous release of acetonitrile and CO_2 in EGA-MS (Figure 3a). The same behavior is reported for different phenylcyanoacetates, including a rate-determining heterolytic decarboxylation step immediately followed by a protonation of the carbanion.[41] Collectively, the results generated on the basis of TGA-FTIR and EGA-MS permit us to propose the activation pathway for TBD-CA shown in **Figure 3d**.

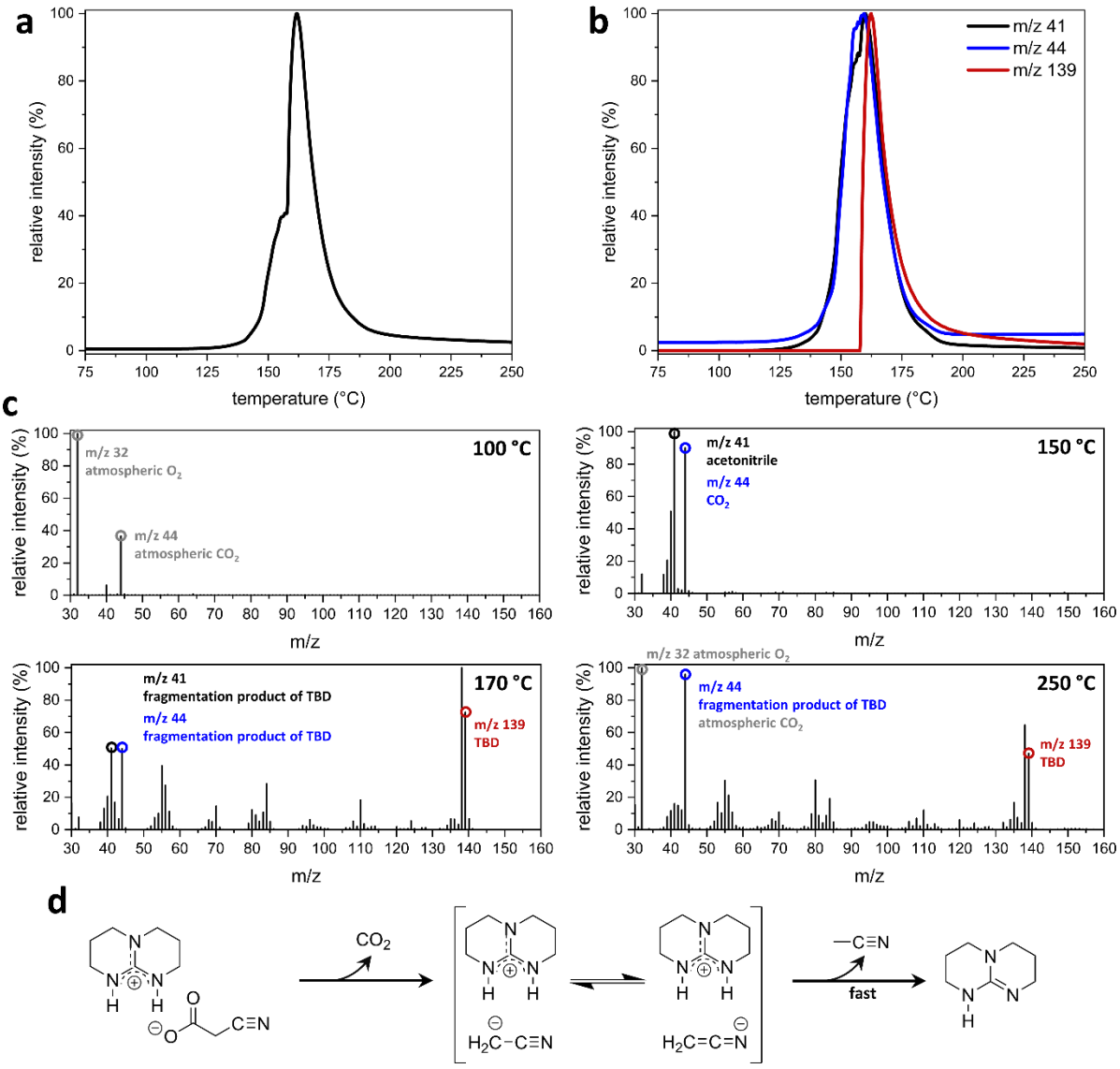

Figure 3. a, b) EGA-MS analysis of TBD-CA including the TIT (a) and the thermal evolution profile of the molecular ion peaks $[M]^+$ of CO_2 (m/z 44), acetonitrile (m/z 41) and TBD (m/z 139) (b). c) Corresponding mass spectra normalized to the respective maximum signal intensity recorded at 100, 150, 170 and 250 °C in scan mode. d) Thermal activation, i.e., decomposition, pathway proposed for TBD-CA.

In conclusion, the synthesized quaternary ammonium salt TBD-CA exhibits characteristics ideal for its application in temperature-controlled reaction catalysis. Immediate decomposition of the thermolabile cyanoacetate protection group enables the controlled and irreversible release of the strong amine base TBD. In the catalysis of numerous polymerization reactions, the conversion of fatty acid feedstocks to biofuel and the catalysis of transesterification reactions in different covalent

adaptable networks, i.e., vitrimers, unmodified TBD is considered as one of the most efficient organic catalysts.[5,13,42] All these examples underline the enormous application potential of the developed thermally latent equivalent TBD-CA presented in this work. Throughout the following sections, the focus is specifically put on the thermolatent catalysis of dynamic transesterification within a covalently cross-linked polymer network.

2.2. Polymer System and Rheological Investigations

The set of so-called click polymerization reactions is characterized by a high tolerance against air and moisture as well as quantitative yields and high rates even under mild reaction conditions.[43] Specifically, the free-radical addition polymerization between a multifunctional thiol and a bifunctional alkene under the formation of thioether links was used. However, to enable a rearrangement of the resulting covalently cross-linked network structure based on dynamic transesterification, both ester moieties and hydroxy groups need to be introduced by an appropriate monomer selection.[4,5,10,13] For network formation, the alkene monomer trimethylolpropane diallyl ether (TMPDE) used was cross-linked with partially esterified pentaerythritol tetrakis(3-mercaptopropionate) (PETMP-75). The pursued radical polymerization mechanism was either initiated by light using ethyl (2,4,6-trimethylbenzoyl) phenylphosphinate (TPO-L) or by temperature using dilauroylperoxide (LP). Chemical structures of the monomers and initiators used are shown in **Figure 4a**.

All samples were prepared in a stoichiometric ratio of thiol groups to allyl moieties and contained the thermally latent transesterification catalyst TBD-CA (readily soluble in both monomers) in a concentration of 7.5 mol% relative to the ester links present. TPO-L (1.0 mol% relative to thiol functions) was used for light-mediated curing and LP (0.25 mol% relative to thiol functions) for thermally induced curing. To verify the polymerization process, FTIR measurements were performed. Independent of the radical initiator applied, the originally present thiol (2568 cm^{-1}) and alkene (3079 cm^{-1}) absorption bands disappeared during curing. On the other hand, hydroxy groups (3463 cm^{-1}) and ester links (1734 cm^{-1}) present in the monomer structures, and essential for the concept of dynamic transesterification, are not affected.[44] Full-scale FTIR spectra prior to and after light-mediated curing via 405 nm LED light in the presence of TPO-L as well as thermal curing by

means of LP (10 min at 60 °C) are provided along with the absorption spectra of the pure monomers in **Figure S6, 7**.

Based on the results obtained by TGA-FTIR (Figure 2) and EGA-MS (Figure 3), temperatures between 125 and 150 °C are needed for the efficient thermally induced on-demand activation of TBD-CA. To ensure that the thiol-ene polymer matrix used is stable during this activation process, TGA of a photo-cured sample (without incorporated TBD-CA) was performed under nitrogen atmosphere at a heating rate of 10 °C min^{-1} (**Figure S8**). Up to a temperature of 300 °C, the mass loss observable is lower than 1 wt%, thus excluding network degradation at the temperature range required for the efficient activation of TBD-CA, i.e., the release of TBD as transesterification catalyst.

For further confirmation, differential scanning calorimetry (DSC) measurements prior to and after activation of TBD-CA incorporated in the photo-cured thiol-ene polymer matrix were carried out at a heating rate of 10 °C min^{-1} (**Figure S9**). Unless otherwise specified, all samples designated as activated in this work were exposed to 130 °C for 15 min. With these measurements, possible degradation reactions in which volatile compounds are not released, the influence of TBD-CA, or rather TBD, on the network stability and possible post-cross-linking processes that might occur during thermal activation can be observed. In general, there are no significant differences between the DSC curves of the unactivated and activated sample and the observable shift in the glass transition temperature from -23 to -22 °C is negligibly small (Figure S9). Hence, it can be concluded that no secondary reactions influencing the pre-existing network properties are provoked by the release of TBD as an active transesterification catalyst. Moreover, the accompanying release of CO_2 and acetonitrile as cleavage of products of the cyanoacetate does not affect the optical appearance of the specimens. Both volatiles are readily dissolved in the polymer matrix or released, preventing the formation of undesirable (micro)bubbles, as proven by microscope images acquired at 5 and 20x magnification prior to and after thermal activation (**Figure S10**). Merely in the highly transparent, colorless, unfilled and undyed samples a marginal yellow coloration can be observed, although such a coloration is not perceptible in any of the applications presented in the following sections.

2.2.1. Rheological Investigations

For examining the influence and latency of TBD-CA, stress relaxation measurements at 70 °C with photo-cured samples activated to varying degrees prior to the measurement were conducted. Sample activation, i.e., on-demand cleavage of TBD-CA within the covalently cross-linked thiol-ene polymer matrix, was carried out at 130 °C for 5, 10 and 15 min using a heating plate. The unactivated reference sample shows a negligible decrease of the normalized relaxation module (G_t/G_0) to 96 % after 175 min, which highlights a remarkable inactivity of TBD-CA in its unactivated state (**Figure 4b**). In comparison, for the 5 min activated sample, a pronounced relaxation to 46 % is already observable after 1 h. By increasing the activation time to 10 and 15 min, relaxation values of 29 and 24 % are reached, respectively, after the same measurement time of 1 h. This drastic change in behavior with respect to the unactivated reference sample is caused by the thermally induced release of TBD as active transesterification catalyst. Depending on the duration of thermal exposure at 130 °C, the amount of catalyst released and thus the rate of dynamic transesterification in terms of topological rearrangements against the applied shear stress are controllable. An additional reference curve was acquired from a sample thermally cured by LP as radical initiator at 60 °C for 10 min (**Figure S11**). Due to the minor relaxation in (G_t/G_0) to 94 % after 175 min at 70 °C, comparable to the photo-cured reference sample, it can be concluded that no significant amounts of TBD are released during the thermal curing process and that the type of radical curing has no substantial influence on the resulting network properties. Overall, the experiments illustrate the outstanding thermal latency of TBD-CA exhibiting a complete inactivity in its unactivated state and at the same time the ability to efficiently catalyze transesterification reactions on-demand at desired rates. Especially with regard to practical applications, the described characteristic offers unique possibilities. Despite the high creep resistance in the unactivated basis state, as typical for conventional covalently cross-linked materials like thermosets and elastomers, on demand, a viscoelastic flow can be generated and exploited for thermomechanical processes such as reshaping, welding or recycling.[15,17]

Subsequently, stress relaxation measurements were performed in a temperature range from 70 to 100 °C on both photo-cured (**Figure 4c**) and thermally cured (**Figure 4d**) specimens that had been fully activated (15 min at 130 °C on a heating plate) in advance. Generally, the stress relaxation process is accelerated toward higher temperatures as the TBD-catalyzed dynamic exchange of covalent bonds and the accompanying reorganization of the network structure against the applied deformation proceeds more rapidly. In respect thereof, a temperature dependence of the characteristic relaxation time (τ) according to the Arrhenius relation ($\tau_{(T)} = \tau_0 \, exp(E_a/RT)$) represents

one of the key characteristics of vitrimers. E_a is the activation energy and R the universal gas constant. Since the decrease in (G_t/G_0) follows a generic exponential behavior, i.e., $(G_t/G_0) = exp(-t/\tau)$, values for τ can be obtained from the experimentally measured stress relaxation curves at the point (G_t/G_0) equals $(1/e)$.[13,45] Independent of the curing procedure, a linear dependency of τ on $(1/T)$ is given in a semilogarithmic scale and thus an Arrhenius-type behavior is confirmed (**Figure 4e**). Such vitreous properties indicate a globally constant, temperature independent network connectivity originating from the associative bond exchange mechanism behind dynamic transesterification.[3,5,13]

Apart from the efficient on-demand catalysis of dynamic transesterification macroscopically visible as a viscoelastic flow, a long-term stability of the inactive basis state, intended to ensure dimensional stability and creep resistance, is of major importance. In this regard, the maintenance in thermal latency of TBD-CA incorporated in photo-cured samples was verified by long-term stress relaxation and creep measurements, carried out in the linear viscoelastic range of the material. Corresponding amplitude sweep measurements are provided in **Figure S12**. At a temperature of 50 °C, even after 60 h no significant stress relaxation is observable and hence dimensional stability can be ensured (**Figure 4f**). By increasing the temperature to 60 °C, gradual stress relaxation starts after about 35 h due to the thermally induced release of TBD. Toward higher temperatures, this trend intensifies and at 90 °C complete relaxation is already achieved within 4 h. Creep measurements performed under a constant shear stress of 3 kPa over 250 min show an elastic deformation of about 0.6 % (**Figure 4g**). At temperatures up to 70 °C, no substantial deviations from this elastic deformation appear and accordingly no creep occurs. However, as the temperature is increased to 80 and 90 °C, the onset of creep can be detected after 175 and 45 min, respectively. In total, TBD-CA in combination with the applied thiol-ene polymer system can be characterized by remarkable thermal latency properties. Based on the results presented, 50 °C can be considered as the maximum application temperature up to which dimensional stability without creep, as common for conventional covalently cross-linked polymers, is ensured. Nevertheless, short-term exceedances of this temperature (e.g., 35 min at 90 °C) provoke no problems for the maintenance of creep resistance.

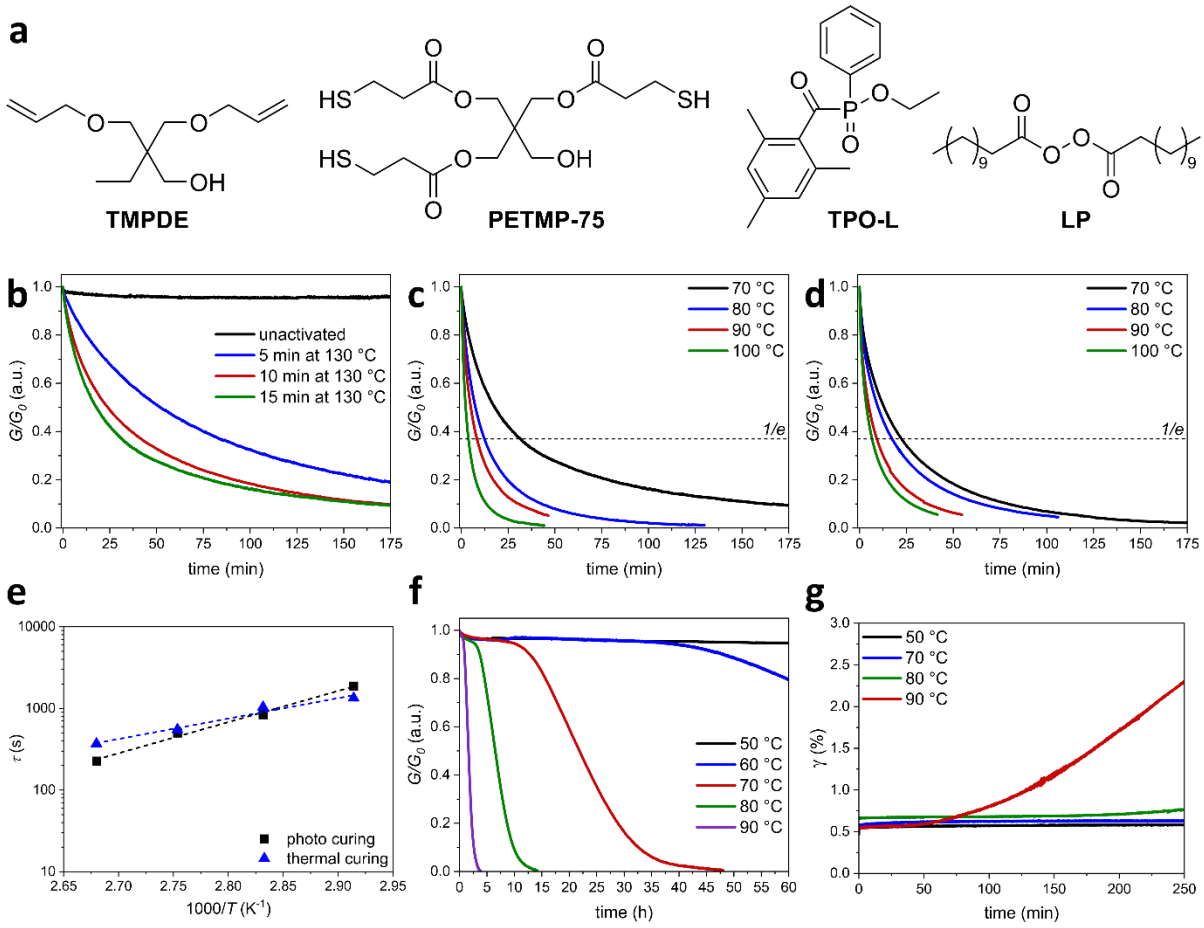

Figure 4. a) Molecular structures of the monomers PETMP-75 (statistically most favored structure) and TMPDE together with TPO-L as radical photoinitiator and LP as radical low-temperature thermal initiator. b) Normalized stress relaxation curves acquired at 70 °C from photo-cured samples before and after thermal activation prior to the measurement at 130 °C for 5, 10 and 15 min. c, d) Stress relaxation data obtained from fully activated photo-cured (c) and thermally cured (d) samples in a temperature range from 70 to 100 °C in 10 °C increments. e) Arrhenius plots of the characteristic relaxation times measured at a decrease of the respective normalized relaxation modulus to 1/e for photo-cured (squares) and thermally cured (triangles) samples. f) Long-term stress relaxation experiments performed with unactivated photo-cured samples in a temperature range from 50 to 90 °C in 10 °C increments. g) Creep measurements carried out under a constant shear stress of 3 kPa at 50, 70, 80 and 90 °C.

2.3. 3D Printing and Spatially Resolved Reshaping

A standard commercially available digital light processing (DLP) 3D printer operating at 405 nm was used for the manufacture of variously shaped objects. Spatially resolved radical thiol-ene polymerization with TPO-L as photoinitiator was performed in a layer-by-layer approach with a constant thickness of 50 µm. To minimize the propagation of scattered light in the resin formulation during the printing process, which impairs the achievable spatial resolution, 0.05 wt% of the orange azo dye 1-(2,4-dimethylphenylazo)-2-naphthol (Sudan II) were added to the thiol-ene resin containing TBD-CA as thermally latent transesterification catalyst. The viscosity of the printing formulation was determined to be 182 mPa·s at a constant shear rate of 300 s^{-1}, which is favorably low for the 3D printing technology applied (**Figure S13**). Every manufactured 3D thiol-ene photopolymer structure was post-cured in a 405 nm curing chamber at room temperature to achieve full conversion of the reactive groups. The emission spectra of all irradiation sources used together with the corresponding intensity values are summarized in **Figure S14**.

For visualization of the outstanding network properties, confirmed by different stress relaxation and creep experiments, a reshaping experiment including the spatially resolved on-demand activation of vitrimeric properties, i.e., dynamic transesterification, was performed (**Figure 5a**). As a first step, only the right arm of the 3 mm thick 3D-printed stick man was heated to 130 °C for 15 min on a heating plate to trigger the spatially resolved cleavage of TBD-CA accompanied by the irreversible release of TBD as highly active base catalyst. Subsequently, both arms were fastened in straight (stretched) position and the entire setup was placed in a convection oven for 6 h at 70 °C. During this heating step, dynamic transesterification catalyzed by TBD takes place in the previously thermally activated right arm of the stick man. The related exchange of covalent bonds leads to a reorganization of the network structure against the applied force, or rather to the predefined straight position. After removing the fixation unit, the stretched covalently cross-linked network of the unactivated left arm containing TBD-CA still in its thermally latent state immediately returned to the entropically more favorable curved shape defined by photopolymerization. On the other hand, the right arm containing TBD released during thermal activation at 130 °C was able to retain its straightened shape caused by a permanent rearrangement of the network topology through base

catalyzed dynamic transesterification. In a following step, also the stick man's left arm was thermally activated (130 °C for 15 min on a heating plate) to illustrate the preserved thermal latency of TBD-CA in this part of the object. Same as before, both arms were stretched, fastened in straight position and stored in a convection oven for 6 h at 70 °C. This time, the left arm was able to retain the predefined straightened shape as well after removing the fixation unit, which can be attributed again to TBD-catalyzed dynamic transesterification and the initiated rearrangement of the covalently cross-linked network structure against the applied force. For demonstrating the repeatability (reversibility) in reorganization of the network topology based on dynamic covalent bond exchange reactions between ester links and hydroxy moieties, both arms were bent downwards (starting from straight position) and fastened. After 3 h at 90 °C and removal of the fixation unit, the position was adopted permanently for both arms. The whole experiment clearly highlights the feasibility of a thermally induced spatiotemporal activation of vitrimeric properties applicable for the repeatable shape definition at the scale of a 3D-printed object.

The achievable printing resolution is depicted by the fabrication of a comb-like structure exhibiting high quality surface properties. Down to a size (diameter) of less than 0.6 mm, bars and holes could be resolved without any difficulty (**Figure S15**). In the absence of Sudan II, it was not possible to manufacture three-dimensional objects because the propagation of scattered light led to extensive polymerization in the vat. As an in Z-direction more sophisticated object, an elephant in the size of 30 mm x 13 mm x 20 mm was 3D-printed. Its originally lifted trunk was permanently shaped to the ground following a multi-step reshaping process based on the exchange of covalent bonds via dynamic transesterification (**Figure 5b**). According to the concept described above, the on-demand decomposition of TBD-CA, i.e., the on-demand release of TBD as an efficient base catalyst for the transesterification process, was previously carried out by a thermal heat treatment (130 °C for 15 min in a convection oven). The entire process comprising four individual steps of reshaping, each performed at 100 °C for 1 h in a convection oven, can be followed in **Figure S16**.

On top of reshaping, the base catalyzed associative exchange between ester links and hydroxy moieties within the applied covalently cross-linked thiol-ene polymer matrix was utilized for welding of circular defects in the center of 3D-printed rectangular test specimens with a thickness of 1.5 mm. Uniaxial tensile testing experiments were performed for determining the efficiency of welding (**Figure 5c**). For the reference fabricated without the defect, a tensile strength of 0.48 ± 0.02 MPa

was determined, which is about 58 % higher compared to the sample with a circular hole in the center (0.20 ± 0.01 MPa). The repair of test specimens with defect was carried out by fitting circular-shaped counterparts, also 3D-printed from the same material, into the hole. Subsequent to cleavage of the thermally latent base catalyst TBD-CA present in the formulation (130 °C for 15 min in a convection oven), welding was performed between two metal plates at 100 °C for 60 h in the same convection oven. During this time period, the interfaces between the two adjacent loose parts are connected by the (re)formation of covalent bonds via TBD-catalyzed dynamic transesterification. Although a boundary line between the two parts is still marginally recognizable, the tensile strength of the reference was restored on average (0.48 ± 0.02 MPa). Thus, excellent welding properties based on the base-catalyzed exchange between ester and hydroxy moieties are evidenced for the developed covalently cross-linked thiol-ene polymer manufactured by 3D printing.

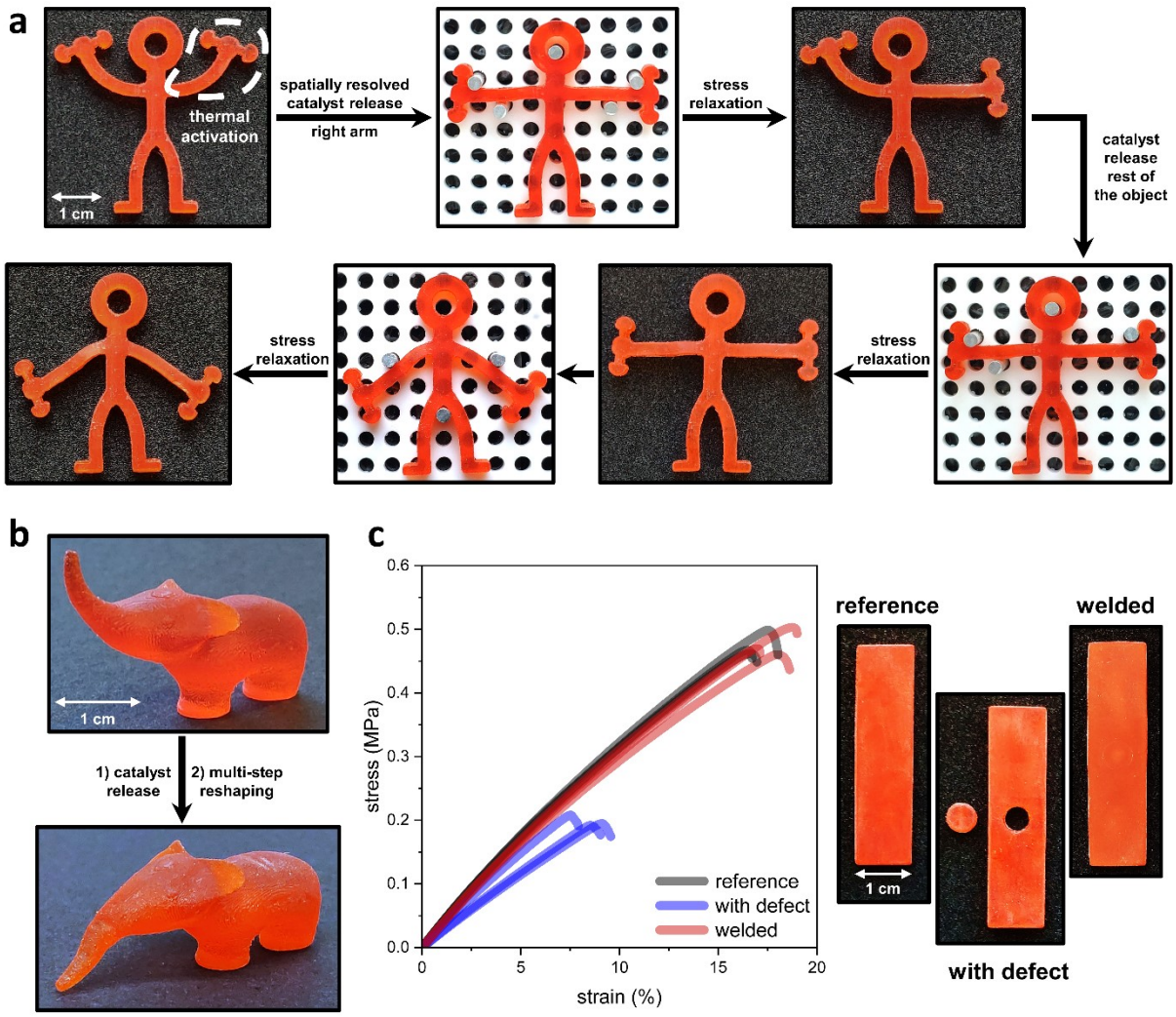

Figure 5. a) Locally controlled and repeated reshaping of a 3D-printed object achieved by the spatially resolved cleavage of the thermally latent base catalyst TBD-CA and a rearrangement of the respective area's network topology via base-catalyzed dynamic transesterification. b) Initial and final state of a 3D-printed object with more sophisticated geometry in a multi-step reshaping experiment carried out after the irreversible heat induced release of TBD from TBD-CA. c) Stress-strain curves in triplicates obtained by tensile testing from 3D-printed samples prior to and after welding a circular defect in addition to a reference fabricated without the defect.

In the literature, the number of 3D-printable vitrimers providing a (spatio)temporal control over their dynamic bond exchange properties is very limited. Due to outstanding curing properties with regard to the DLP printing technology, most commonly di- or multifunctional acrylates are applied as (co)monomers.[21,22,46] However, this category of polymer networks suffers from internal stresses resulting from a pronounced cure shrinkage arising during photopolymerization.[47] As a consequence, for the generated covalently cross-linked latent vitrimer networks, an undesired stress relaxation, i.e., creep, can be observed even before their actual activation, reflecting a lack in dimensional stability.[21,22] Owing to the herein introduced photocurable monomer combination between a multifunctional thiol and a bifunctional alkene, the described constraint is overcome. 3D-printed creep-resistant objects equipped with spatially resolved on-demand activatable vitrimeric properties (Figure 4) were produced and exploited for reshaping and welding (Figure 5) by the dynamic exchange of covalent bonds within the cross-linked network topology.

2.4. Reshaping of Particulate and Fiber-Reinforced Composites

Overall, the vast majority of vitrimeric polymers enabling a temporal control in terms of their dynamic bond exchange behavior are based on photolatent catalysis.[18–23] Substantial shortcomings appear in their practical application as the photolatent effect can be only maintained under the exclusion of (day)light. In addition, the geometry of the components to be produced is seriously limited as often, material thicknesses beyond the penetration depth of the light, essential to activate the photolatent catalyst, are required. Based on the presented development of TBD-CA as efficient thermally latent base catalyst, samples exhibiting latent vitrimeric properties in any geometry applicable and independent on the present light conditions can be manufactured. Since the on-demand catalysis of dynamic transesterification within a covalently cross-linked polymer matrix is

simply triggerable by an increase in temperature, the whole user friendliness is considerably improved compared to the established photolatent systems. Furthermore, our approach allows the novelty of an unrestricted use of fillers and colorants as an optical transparency is not needed for catalyst activation. In order to emphasize this considerable advantage, reshaping experiments with selected classes of composites were performed.

First, magnetic Fe_3O_4 nanoparticles (15 wt% relative to the total mass) were dispersed in the thiol-ene formulation containing TBD-CA as thermally latent transesterification catalyst and LP as low-temperature radical polymerization initiator. After curing performed at 60 °C for 10 min, a black colored, opaque and 1 mm thick test specimen of rectangular shape was obtained and applied in a magnetically assisted reshaping experiment (**Figure 6a**). Steered by means of two neodymium rod magnets, the specimen could be freely aligned in levitation. Subsequent to the thermally induced activation process (130 °C for 15 min on a heating plate), i.e., the irreversible release of TBD as efficient transesterification catalyst originating from TBD-CA, a spherical neodymium magnet was used to convert the originally straight specimen into a curved shape. Fixated solely through the magnetic interaction between the test specimen and the spherical magnet, the experimental setup was stored for 3 h at 90 °C in a convection oven. During this heating period, a reorganization of the network structure against the applied deformation entailed by the TBD-catalyzed dynamic exchange of covalent bonds took place. Therefore, the curved shape had been permanently preserved, even after the spherical magnet was removed. Conclusively, the magnetic response of the test specimen was not affected by the thermally induced cleavage of TBD-CA and the reorganization of the network topology via dynamic transesterification.

As a second example, the introduced thermally latent vitrimer was used as a matrix material to manufacture a fiber-reinforced composite. Therefore, a 500 g m^{-2} flax fiber fabric was impregnated with the vitrimer system at a temperature of 40 °C in a vacuum assisted resin infusion (VARI) process. The applied fabrication setup along with a detailed schematic representation is shown in **Figure S17**. Immediately after complete saturation of the rectangular flax fiber fabric (210 mm x 110 mm), the thiol-ene resin was cured at 60 °C for 15 min facilitated by LP as low-temperature radical polymerization initiator. Through the mirror-like surface of the resulting about 1 mm thick composite, no visible defects or inhomogeneities were observed in the textile's opaque 4/4 twill structure (**Figure S18**), indicating a good infusion behavior of the matrix system.

The fiber volume fraction of the composite was determined to be 36 %, which is within the expected range for VARI processes, although a tendency toward lower saturation levels of the fiber bundles may be assumed.[48] For the corresponding reshaping experiment depicted in **Figure 6b**, the composite was cut into a 20 mm wide stripe with a length of 210 mm.

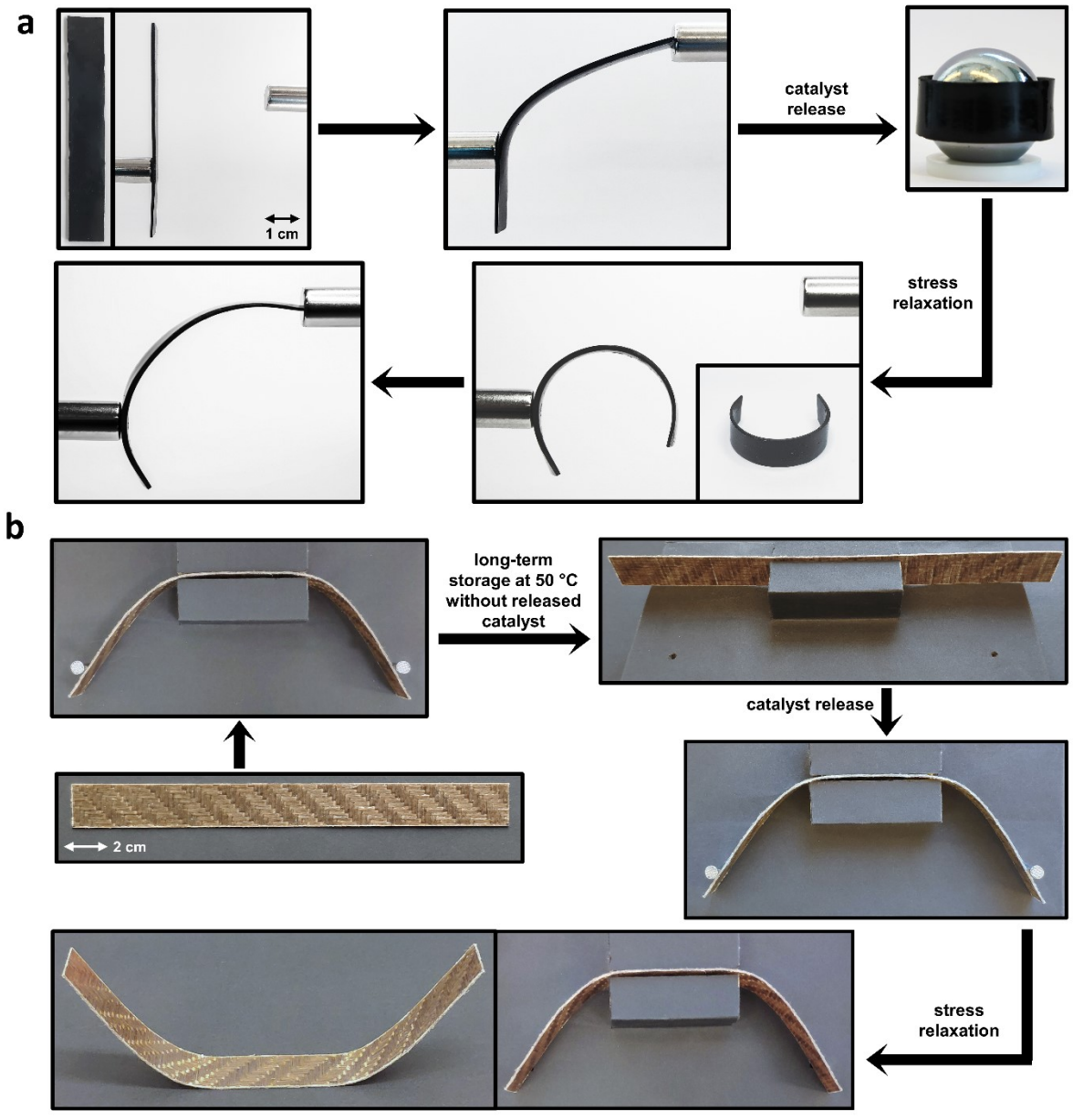

Figure 6. Permanent reshaping of composite structures based on the temperature induced cleavage of TBD-CA as thermally latent base catalyst in the reorganization process of the covalently cross-linked network structure via dynamic transesterification. a) Magnetic assisted reshaping of a Fe_3O_4 particulate composite. b) Reshaping of a fiber-reinforced composite.

First, the specimen in its unactivated state was clamped into a customized fixture by which two bends with an approximate inner angle of 45° were introduced into the originally straight shape. To recreate a practical application example under load at elevated temperatures, the whole setup was stored at 50 °C in a convection oven. Due to the maintained thermal latency of TBD-CA at this temperature (Figure 4f), base-catalyzed dynamic transesterification and a reorganization of the network structure cannot occur. Consequently, no permanent deformation of the specimen could be observed even after 50 h, as typical for permanently cross-linked polymers.[1,15,17] However, by heating the fiber-reinforced composite in a convection oven at 130 °C for 15 min, TBD as active transesterification catalyst was released on demand. After the specimen was clamped into the fixture again and exposed to 100 °C in a convection oven for 3 h, the predefined double angled shape was permanently adopted. Despite the proven dimensional stability of our material in its unactivated state, a viscous flow caused by the TBD-catalyzed dynamic exchange between ester links and hydroxy groups could be generated on demand and exploited for thermochemical reshaping.

3. Conclusion

Collectively, the straight-forward one-step synthesis of a thermally latent catalyst for the design of a new generation of dynamic polymer networks has been shown. The catalyst's unprecedented ability to switch from a complete latency in its unactivated state to a highly efficient basic species simply by temperature offers a tremendous potential for future applications in the general area of temperature-controlled reaction catalysis. Incorporated in a three-dimensional covalently cross-linked thiol-ene polymer containing ester links as well as hydroxy moieties, creep resistance is guaranteed. However, on demand, a (spatially resolved) onset of base-catalyzed dynamic transesterification can be triggered by a temperature increase and the accompanied release of the catalyzing species. The resulting viscoelastic behavior has been exploited for thermomechanical reshaping and welding experiments. By following a photo-induced curing of the thiol-ene resin, geometrically demanding objects have been fabricated by DLP 3D printing technology. The versatility in application was further demonstrated by the concurrent possibility of thermal radical curing, which allows the fabrication of highly filled objects such as any kind of composite material. Due to the purely thermally inducible release of the transesterification catalyst, no limitations exist with regard to the object geometry and the use of fillers or dyes. In addition, compared to photolatent

vitrimer systems, manufactured objects can be applied regardless of light conditions. Overall, our outlined approach provides a novel fundamental building block for the unrestricted development of numerous creep resistant vitrimer systems based on the application of a thermally latent catalyst. A possible area for immediate implementation can be found in soft robotics. Furthermore, there is a great potential to realize numerous engineering applications in the future through structural modifications of the thermolatent catalyst, i.e., a targeted increase or decrease of the activation temperature by a directed variation of the anion (carboxylic acid) applied.

Supporting Information

Supporting Information is available from the Wiley Online Library or from the author.

Acknowledgements

We would like to thank Dr. Elisabeth Rossegger as well as Prof. Thomas Grießer from the Institute of Chemistry of Polymeric Materials, Montanuniversität Leoben, for their helpful advice regarding DLP 3D printing. Additionally, we would like to thank Bruno Bock (Marschacht, Germany) for the custom synthesis of the thiol crosslinker (PETMP-75).

The research work was performed within the COMET-Module project “Chemitecture” (project-no.: 21647048) at the Polymer Competence Center Leoben GmbH (PCCL, Austria) within the framework of the COMET-program of the Federal Ministry for Climate Action, Environment, Energy, Mobility, Innovation and Technology and the Federal Ministry for Digital and Economic Affairs with contributions by Montanuniversität Leoben. The PCCL is funded by the Austrian Government and the State Governments of Styria, Lower Austria and Upper Austria.

Received: ((will be filled in by the editorial staff))
Revised: ((will be filled in by the editorial staff))
Published online: ((will be filled in by the editorial staff))

References

[1] D. Ratna, *Recent Advances and Applications of Thermoset Resins*, Elsevier, Amsterdam, NL, **2022**.

[2] T. Kaiser, *Prog. Polym. Sci.* **1989**, *14*, 373.

[3] J. M. Winne, L. Leibler, F. E. Du Prez, *Polym. Chem.* **2019**, *10*, 6091.

[4] M. Podgórski, B. D. Fairbanks, B. E. Kirkpatrick, M. McBride, A. Martinez, A. Dobson, N. J. Bongiardina, C. N. Bowman, *Adv. Mater.* **2020**, *32*, 1906876.

[5] W. Alabiso, S. Schlögl, *Polymers* **2020**, *12*, 1660.

[6] L. I. Farfan-Cabrera, E. A. Gallardo-Hernández, J. Pérez-González, *Tribology International* **2017**, *116*, 1.

[7] a) V. Chaudhary, F. Ahmad, *Polym. Test.* **2020**, *91*, 106792; b) T. Hassan, A. Salam, A. Khan, S. U. Khan, H. Khanzada, M. Wasim, M. Q. Khan, I. S. Kim, *J. Polym. Res.* **2021**, *28*, 1; c) R. Jeyapragash, V. Srinivasan, S. Sathiyamurthy, *Mater. Today Proc.* **2020**, *22*, 1223; d) V. Schenk, K. Labastie, M. Destarac, P. Olivier, M. Guerre, *Mater. Adv.* **2022**, *3*, 8012; e) B. Seers, R. Tomlinson, P. Fairclough, *Polym. Compos.* **2021**, *42*, 1631; f) K. Yu, Q. Shi, M. L. Dunn, T. Wang, H. J. Qi, *Adv. Funct. Mater.* **2016**, *26*, 6098.

[8] B. Krishnakumar, R. P. Sanka, W. H. Binder, V. Parthasarthy, S. Rana, N. Karak, *Chem. Eng. J.* **2020**, *385*, 123820.

[9] C. J. Kloxin, C. N. Bowman, *Chem. Soc. Rev.* **2013**, *42*, 7161.

[10] W. Denissen, J. M. Winne, F. E. Du Prez, *Chem. Sci.* **2016**, *7*, 30.

[11] D. Montarnal, M. Capelot, F. Tournilhac, L. Leibler, *Science* **2011**, *334*, 965.

[12] a) M. Giebler, C. Sperling, S. Kaiser, I. Duretek, S. Schlögl, *Polymers* **2020**, *12*, 1148; b) Y. Jin, Z. Lei, P. Taynton, S. Huang, W. Zhang, *Matter* **2019**, *1*, 1456.

[13] T. Liu, B. Zhao, J. Zhang, *Polymer* **2020**, *194*, 122392.

[14] M. Guerre, C. Taplan, J. M. Winne, F. E. Du Prez, *Chem. Sci.* **2020**, *11*, 4855.

[15] Y. Liu, Z. Tang, D. Wang, S. Wu, B. Guo, *J. Mater. Chem. A* **2019**, *7*, 26867.

[16] F. van Lijsebetten, K. de Bruycker, J. M. Winne, F. E. Du Prez, *ACS Macro Lett.* **2022**, *11*, 919.

[17] F. van Lijsebetten, T. Debsharma, J. M. Winne, F. E. Du Prez, *Angew. Chem., Int. Ed.* **2022**, *61*, e202210405.

[18] B. T. Worrell, M. K. McBride, G. B. Lyon, L. M. Cox, C. Wang, S. Mavila, C.-H. Lim, H. M. Coley, C. B. Musgrave, Y. Ding et al., *Nat. Commun.* **2018**, *9*, 2804.

[19] D. Reisinger, K. Dietliker, M. Sangermano, S. Schlögl, *Polym. Chem.* **2022**, *13*, 1169.

[20] D. Reisinger, S. Kaiser, E. Rossegger, W. Alabiso, B. Rieger, S. Schlögl, *Angew. Chem., Int. Ed.* **2021**, *60*, 14302.

[21] C. Dertnig, G. La Guedes de Cruz, D. Neshchadin, S. Schlögl, T. Griesser, *Angew. Chem., Int. Ed.* **2022**, e202215525.

[22] E. Rossegger, K. Moazzen, M. Fleisch, S. Schlögl, *Polym. Chem.* **2021**, *12*, 3077.

[23] W. Zou, B. Jin, Y. Wu, H. Song, Y. Luo, F. Huang, J. Qian, Q. Zhao, T. Xie, *Sci. Adv.* **2020**, *6*, eaaz2362.

[24] W. C. P. Tsang, A. Bell, (Sumitomo Bakelite Co Ltd), *US009115300B2* **2015**.

[25] a) A. Kobayashi, F. Kobayashi, T. Ebina, R. Ishii, T. Nakamura, T. T. Nge, T. Yamada, A. Shiraishi, T. Yamashita, *J. Photopolym. Sci. Technol.* **2018**, *31*, 101; b) S. B. Lee, T. Takata, T. Endo, *Macromolecules* **1991**, *24*, 2689.

[26] H. Salmi, X. Allonas, C. Ley, A. Defoin, A. Ak, *Polym. Chem.* **2014**, *5*, 6577.

[27] K. Arimitsu, R. Endo, *J. Photopolym. Sci. Technol.* **2010**, *23*, 135.

[28] C. A. de La Lastra, A. Nieto, V. Motilva, M. J. Martín, J. M. Herrerías, F. Cabré, D. Mauleón, *Inflammation Res.* **2000**, *49*, 627.

[29] T. Ando, Y. Fujimoto, S. Morisaki, *J. Hazard. Mater.* **1991**, *28*, 251.

[30] A. J. Belsky, P. G. Maiella, T. B. Brill, *J. Phys. Chem. A* **1999**, *103*, 4253.

[31] D. J. Darensbourg, J. A. Chojnacki, E. V. Atnip, *J. Am. Chem. Soc.* **1993**, *115*, 4675.

[32] S. T. Graul, R. R. Squires, *J. Am. Chem. Soc.* **1990**, *112*, 2517.

[33] J. Li, G. N. Khairallah, V. Steinmetz, P. Maitre, R. A. J. O'Hair, *Dalton Trans.* **2015**, *44*, 9230.

[34] a) S. Moins, C. Henoumont, J. de Winter, A. Khalil, S. Laurent, S. Cammas-Marion, O. Coulembier, *Polym. Chem.* **2018**, *9*, 1840; b) X. Sun, J. P. Gao, Z. Y. Wang, *J. Am. Chem. Soc.* **2008**, *130*, 8130.

[35] I. D. Reva, S. G. Stepanian, L. Adamowicz, R. Fausto, *J. Phys. Chem. A* **2003**, *107*, 6351.

[36] a) E. V. Fufachev, B. M. Weckhuysen, P. C. A. Bruijnincx, *ChemSusChem* **2021**, *14*, 2710; b) Y. Maréchal, *J. Chem. Phys.* **1987**, *87*, 6344.

[37] M. R. Islam, Z. Guo, D. Rutman, T. J. Benson, *RSC Adv.* **2013**, *3*, 24247.

[38] B. Brzezinski, G. Schroeder, V. I. Rybachenko, L. I. Kozhevina, V. V. Kovalenko, *J. Mol. Struct.* **2000**, *516*, 123.

[39] John Wiley & Sons, Inc., Spectrum ID: 8_LMCM-39693-350S.

[40] Z. Tian, S. R. Kass, *Chem. Rev.* **2013**, *113*, 6986.

[41] T. S. Straub, M. L. Bender, *J. Am. Chem. Soc.* **1972**, *94*, 8875.

[42] J. Borton, F. D. Nato Lopez, L. Doan, W. E. Holmes, T. J. Benson, *Energy Fuels* **2019**, *33*, 3322.

[43] C. E. Hoyle, C. N. Bowman, *Angew. Chem., Int. Ed.* **2010**, *49*, 1540.

[44] R. Nagarjuna, M. S. M. Saifullah, R. Ganesan, *RSC Adv.* **2018**, *8*, 11403.

[45] M. Capelot, M. M. Unterlass, F. Tournilhac, L. Leibler, *ACS Macro Lett.* **2012**, *1*, 789.

[46] B. Krishna Kumar, T. J. Dickens, *J. Appl. Polym. Sci.* **2023**, *140*, e53304.

[47] G. Sun, X. Wu, R. Liu, *Prog. Org. Coat.* **2021**, *155*, 106229.

[48] M. Neitzel, P. Mitschang, U. P. Breuer (Eds.) *Handbuch Verbundwerkstoffe*. *Werkstoffe, Verarbeitung, Anwendung*, Hanser, München, DE, **2014**.

A thermally latent ammonium salt is synthesized and its on-demand release of a strong base is exploited for the selective activation of bond exchange reactions in covalently crosslinked polymers. The thermally triggered (and local) change from a creep resistant behavior to a highly dynamic polymer network is demonstrated and applied for the reshaping/welding of 3D-printed objects and various composite structures.

D. Reisinger, M. U. Kriehuber, M. Bender, D. Bautista-Anguís, B. Rieger and S. Schlögl*

Thermally Latent Bases in Dynamic Covalent Polymer Networks and their Emerging Applications